Geographic Atrophy Progression Is Associated With Choriocapillaris Flow Deficits Measured With Optical Coherence Tomographic Angiography

Qi Sheng You,[1,3] Acner Camino,[1] Jie Wang,[1,2] Yukun Guo,[1] Christina J. Flaxel,[1] Thomas S. Hwang,[1] David Huang,[1] Yali Jia,[1,2] and Steven T. Bailey[1]

[1]Casey Eye Institute, Oregon Health and Science University, Portland, Oregon, United States
[2]Department of Biomedical Engineering, Oregon Health & Science University, Portland, Oregon, United States
[3]Kresge Eye Institute, Detroit Medical Center, Wayne State University, Detroit, Michigan, United States

PURPOSE. The purpose of this study was to assess the associations between baseline choriocapillaris (CC) flow deficits and geographic atrophy (GA) progression.

METHODS. In this prospective cohort study, patients with GA underwent 3×3-mm macular spectral-domain optical coherence tomographic angiography (OCTA) at baseline and follow-up visits. Annual GA enlargement rate was defined as change of square root of GA area in 12 months. Shadow areas due to iris, media opacity, retinal vessels, and drusen were excluded. CC vessel density (CC-VD) in non-GA areas was measured using a validated machine-learning-based algorithm. Low perfusion area (LPA) was defined as capillary density below the 0.1 percentile threshold of the same location of 40 normal healthy control eye. Focal perfusion loss (FPL) was defined as percentage of CC loss within LPA compared with normal controls.

RESULTS. Ten patients with GA were enrolled and followed for 26 months on average. At baseline, the mean GA area was 0.84 ± 0.70 mm^2. The mean CC-VD was $44.5 \pm 15.2\%$, the mean LPA was 4.29 ± 2.6 mm^2, and the mean FPL was $50.4 \pm 28.2\%$. The annual GA enlargement rate was significantly associated with baseline CC-VD ($r = -0.816$, $P = 0.004$), LPA ($r = 0.809$, $P = 0.005$), and FPL ($r = 0.800$, $P = 0.005$), but not with age ($r = 0.008$, $P = 0.98$) and GA area ($r = -0.362$, $P = 0.30$).

CONCLUSIONS. Baseline CC flow deficits were significantly associated with a faster GA enlargement over the course of 1 year, suggesting the choriocapillaris perfusion outside of a GA area may play a role in GA progression.

Keywords: geographic atrophy, optical coherence tomography angiography, age-related macular degeneration

Geographic atrophy (GA) secondary to age-related macular degeneration (AMD) is characterized by loss of photoreceptors, retinal pigment epithelium (RPE), and choriocapillaris.[1] GA is a significant cause of severe vision loss, accounting for approximately 20% of all cases of legal blindness in North America and affecting more than 8 million people worldwide.[1,2] A GA lesion usually starts in the extrafoveal area and enlarges progressively to involve central fovea and leads to severe vision loss.[3,4] There is a limited understanding of the mechanism of GA development and progression. Previous studies have suggested oxidative stress, inflammation, and ischemia may all play roles in its pathogenesis.[5–8]

Optical coherence tomographic angiography (OCTA) is a novel noninvasive imaging method. Using flowing blood cells as intrinsic contrast, OCTA enables us to image retinal and choroidal blood vessels at the capillary level.[9] Recent studies on GA with OCTA have demonstrated retinal and choroidal blood flow impairment.[10–15] Using projection resolved OCTA (PR-OCTA), we recently reported significant reduced vessel densities in retinal plexuses in GA eyes compared with normal healthy controls.[12] Sacconi demonstrated that choriocapillaris (CC) flow impairment could be observed with a spectral domain OCTA around the atrophic lesions in GA eyes.[14] Using a swept source OCTA, Nassisi also reported a significant impairment of CC flow in the zones immediately surrounding the GA lesions.[10] These cross-sectional studies suggested CC alterations might be relevant to the progression of GA. In more recent longitudinal studies, researchers reported significant correlations between swept source OCTA measured CC flow deficits and GA enlargement rate over 1 year.[11,13,16]

Measuring CC could be technically challenging due to artifacts from motion, projections, segmentation errors, and shadows.[17] Motion artifacts due to saccades, ocular tremors, or drift are noise components difficult to subtract.[18] Projections of the overlying retinal flow could induce significant inaccuracies in CC quantifications.[19] Segmentation errors of the very thin CC layer can also produce incorrect measurements.[20,21] Shadow effects caused by large

drusen, retinal vessels, vitreous floaters, and pupil vignetting could artifactually attenuate the CC signal.[22,23] Previously, we developed comprehensive artifacts removal techniques, including projection-resolved OCTA (PR-OCCTA),[19,24] bidirectional graph search for accurate segmentation,[25] and iterative regression-based bulk motion subtraction.[18] In addition to these techniques, we recently developed a machine-learning-based shadow removal algorithm to improve the CC flow measurement after excluding the impact of drusen, retinal vessels, vitreous floaters, and iris.[22,26] In the current prospective cohort study, we aimed to assess the associations between baseline CC flow deficits and GA progression rates using our custom OCTA algorithms designed to mitigate artifact on CC angiograms.

METHODS

This prospective cohort study adhered to the tenets of the Declaration of Helsinki and was conducted in compliance with the Health Insurance Portability and Accountability Act. The institutional review board at Oregon Health and Science University approved the study and written informed consent was obtained from each participant.

The inclusion and exclusion criteria of the study participants have been reported recently.[12] Briefly, inclusion criteria for patients with GA were an age of 50+ years and diagnosis of GA secondary to AMD in at least one eye. GA was defined as sharply demarcated atrophic lesions of at least 175 μm with increased visibility of choroidal vessels. The diagnosis of GA was confirmed by both hypoautofluorescence on fundus autofluorescence (FAF) image and OCT scans (Spectralis Heidelberg Engineering, Heidelberg, Germany) demonstrating congruent loss of photoreceptors and RPE and hypertransmission of an OCT signal into the choroid. The exclusion criteria included a history of choroidal or retinal neovascularization, previous intraocular surgery, except cataract surgery, any other macular disease, such as significant epiretinal membrane or vitreomacular traction syndrome, refractive error greater than −6 or +3 diopters and media opacities that precludes a high-quality OCTA scan.

Each participant underwent a comprehensive ocular examination, including axial length measurement (IOL master 500; Carl Zeiss Meditec, Dublin, CA, USA), early treatment of diabetic retinopathy study (ETDRS) visual acuity testing, intraocular pressure, dilated fundus examination, fundus photography (Zeiss FF450 plus, Carl Zeiss Meditec, USA), FAF (Spectralis HRA + OCT; Spectralis, Heidelberg Engineering), and OCTA.

After mydriasis, OCTA was obtained for both baseline and follow-up visits, using a commercially available spectral-domain instrument, RTVue XR Avanti (Optovue, Inc.), with a center wavelength of 840 nm and an axial scan rate of 70 kHz. The 3 × 3-mm scans centered at the fovea were acquired with the embedded real-time eye tracking function turned on to minimize micro saccade motion artifacts. A repeat scan was performed on the same visit with the patient sitting up and re-positioned to assess the measurement repeatability. Blood flow signal was detected using the commercial version of split-spectrum amplitude decorrelation angiography (SSADA) algorithm by comparing consecutive B-scans at the same location.[9] The AngioVue software uses an orthogonal registration algorithm to register the two-perpendicular (vertical-priority and horizontal-priority) raster volumes to produce a merged 3D OCT angiogram.

The merged volumetric angiograms were then exported for custom processing using our laboratory developed software. Baseline scans were excluded if images were out of focus, significant motion artifacts were present, or if signal strength index (SSI) was less than 50.

The interfaces among the vitreous/inner limiting membrane, outer plexiform layer/outer nuclear layer, RPE, and Bruch's membrane/CC were auto-segmented on structural OCT B scans using a validated directional graph search method.[25] These segmentations were manually reviewed and adjusted where necessary. An iterative regression-based bulk motion subtraction algorithm was applied to subtract bulk motion artifacts.[18] A reflectance-based PR-OCTA algorithm was used to remove projection artifacts of inner retinal flow onto CC layer.[19] En face angiograms of CC were generated by maximum projection of a slab located between 10 and 18 μm below the Bruch's membrane, as reported recently.[22,27] An automated drusen detection algorithm was applied, as described previously.[28] Shadow areas due to iris, media opacity, retinal vessels, or drusen were automatically detected using a validated deep-learning algorithm.[26]

GA area on baseline and last follow-up visit was segmented manually by a human grader using the en face mean projections of the reflectance choroidal and RPE slabs defined using the RPE and Bruch's membrane layer boundaries segmented automatically by a validated algorithm. The cross-sectional B scans were referred to when segmenting GA on en face images. The characteristic of GA on cross-sectional B scans included loss of RPE and photorecepters and hypertransmission of light, as described in the Classification Atrophy Meetings literature.[29] The capillary density was defined as the percentage of vascular pixels through the whole en face angiograms. The CC vessel density (CC-VD) outside GA area was calculated after excluding the GA area and shadow area.

Considering the CC-VD is not evenly distributed across the macular area, we calculated low perfusion area (LPA) and focal perfusion loss (FPL) using a position point reference map generated from 40 normal healthy controls, as reported recently.[12,22] The image of GA eyes and the reference map were registered for location wise comparison (Fig. 1). An expert grader manually selected the foveal center, and all local density maps were registered by rigid translations to make their foveal-center positions overlap. LPA was defined as superpixel ($\geq$15 contiguous pixels) capillary density below the 0.1 percentile threshold of the same location in 40 normal healthy control eyes (i.e. threshold $(x,y) = CC_{ref} (x,y)-3.1 CC_{std} (x,y)$). FPL was defined as percentage of CC loss within LPA compared to normal controls (i.e. $FPL = \frac{\sum LPA((CCref(x,y)-CC(x,y))}{\sum CCref(x,y)}$). CC loss was the difference between measured CC (x,y) and the reference $CC_{ref} (x,y)$ (i.e. CC loss = $CC_{ref} (x,y)$-CC (x,y)).

Statistical analysis was performed using Statistical Package for Social Sciences software (SPSS for Windows, version 25.0; IBM SPSS Inc., Chicago, IL, USA). Intraclass correlation coefficient (ICC) was calculated to assess the intra-visit repeatability. Among the two repeat scans, the scan with a higher SSI was selected for the final statistical analysis. Descriptive statistics included mean, standard deviation (SD), range, and percentages were presented where appropriate. Paired Student's *t* test was used to compare the SSI and Q value of the baseline and follow-visit scans. Pearson correlation analysis was used to analyze the correlation between baseline CC-VD, LPA, FPL, and GA area. Annual
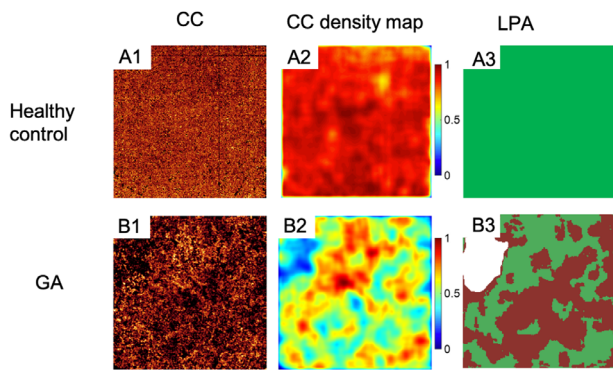
Figure 1. Examples of en face choriocapillaris (CC) optical coherence tomography angiography (OCTA), CC density map, and low perfusion area; in a healthy control and a case with geographic atrophy. (A1) CC of a healthy control; (B1) CC density map of the healthy control; (C1) low perfusion area is not detected in this healthy eye. (B1) Reduced CC in eye with geographic atrophy (GA); (B2) CC density map in the eye with GA; (B3) low perfusion area (red) detected along with areas of normal perfusion (green) in eye with GA. Region of GA (white) is excluded for quantitative analysis.

GA enlargement rate was defined as change of square root of GA area over 12 months. The associations among GA enlargement rate and baseline age, GA area, CC-VD, LPA and FPL were assessed using Pearson correlation analysis. All *P* values were 2-sided and considered statistically significant if the value was less than 0.05.

RESULTS

Ten patients with GA (7 men) were included into the study. At enrollment, the mean age of the study participants was 81 $\pm$ 9 (mean $\pm$ standard deviation, range = 66–95) years. The mean axial length of the study eyes was 23.84 $\pm$ 0.85 (range = 22.06–24.75) mm. The mean visual acuity was 76 $\pm$ 8 (range = 62–89) ETDRS letters. GA lesions were multifocal in seven eyes and involved the foveal center in two eyes. Reticular pseudodrusen were found in two eyes. Fundus autofluorescence patterns were diffuse or banded in two eyes, focal in five eyes, patchy in one eye, and none in two eyes. The fellow eyes had choroidal neovascularization in eight eyes and GA in two eyes.

Nine eyes had intra-visit repeat scans at both baseline or follow-up. The within visit repeatability (ICC) scores for these scans was 0.958, 0.947, and 0.955 for CC-VD, LPA, and FPL measurements, respectively. The mean GA area at baseline was 0.84 $\pm$ 0.70 (range = 0.03–2.25) mm^2. The mean shadow area was 1.12 $\pm$ 0.63 (range = 0.27–2.42) mm^2. After GA areas and shadow areas were excluded, the mean CC-VD was 44.5 $\pm$ 15.2 % (range = 16.5%–67.5%). The mean LPA was 4.29 $\pm$ 2.6 (range = 0.48–7.49) mm^2. The mean FPL was 50.4 $\pm$ 28.2% (range = 5.4%–82.4%). The baseline GA area was not significantly associated with CC-VD (correlation coefficient r = 0.291, *P* = 0.41), nor with LPA (r = −0.387, *P* = 0.27) or FPL (r = −0.340, *P* = 0.34).

Patients with GA were followed an average of 26 months (range = 12–51 months). The mean SSI was 58.1 $\pm$ 7.5 at baseline and 61.0 $\pm$ 7.7 (*P* = 0.34) at follow-up. The mean Q scores for these scans were 6 $\pm$ 1.8 and 7 $\pm$ 1.7 (*P* = 0.19)
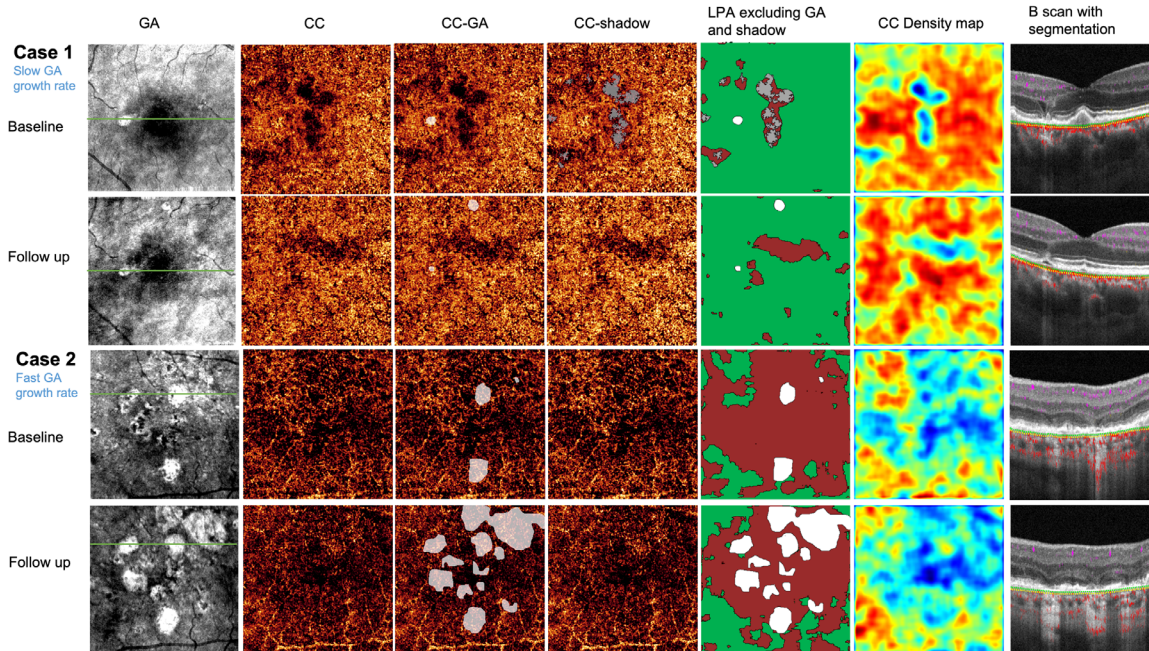
Figure 2. Greater baseline choriocapillaris low perfusion area (LPA) is associated with faster geographic atrophy (GA) annual enlargement rate. Projected (first column) OCT slab demonstrating GA as white areas. Choriocapillaris (CC) optical coherence tomography angiography (OCTA) in second column. GA areas are presented in white over CC OCTA (third column). Shadow artifacts are presented in gray over CC OCTA (fourth column). Normal CC perfusion labeled in green, GA in white, shadow artifact in gray, and LPA in red (fifth[h] column). The flow CC density map shows lower CC density as blue area and higher CC flow density as red area (sixth column). Cross-sectional structural OCTA shows layer segmentation (seventh column). In case 1, the baseline LPA outside GA area was 0.48 mm^2 and the focal perfusion loss (FPL) was 5.4%. The GA enlargement rate was 0.06 mm/year. In case 2, the baseline LPA and FPL outside the GA area was 6.91 mm^2 and 79.2%, respectively. The GA enlargement rate was 0.51 mm/year.
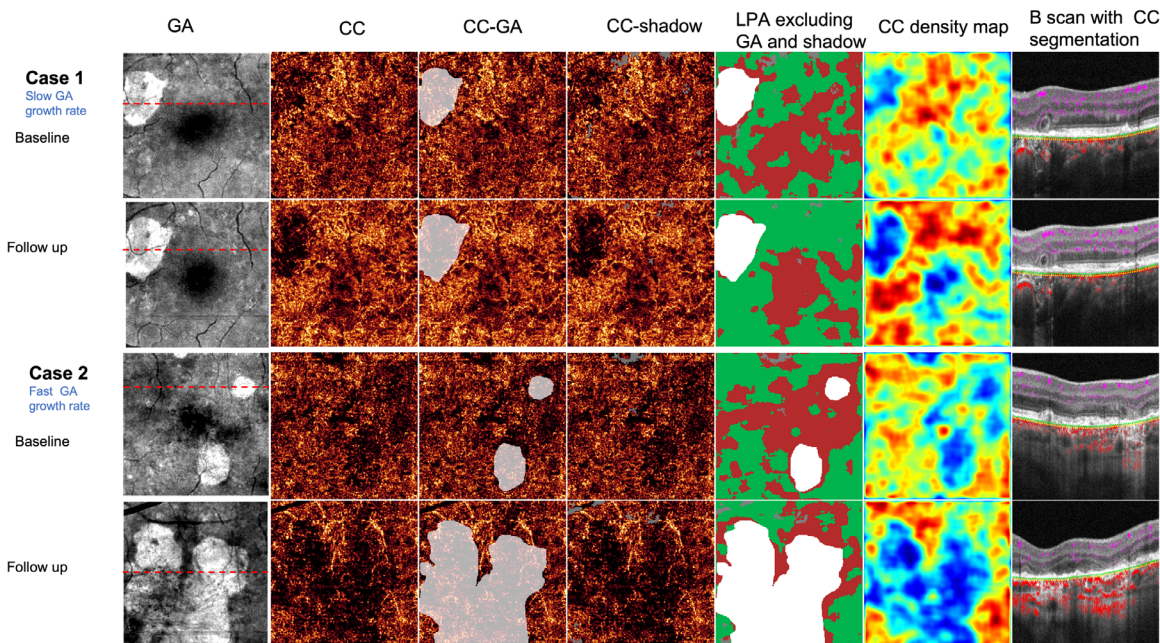
FIGURE 3. Slow (0.05 mm/year) geographic atrophy growth rate (case 3) compared to faster (0.19 mm/year) geographic atrophy growth rate (case 4). Projected (first column) OCT slab demonstrating GA as white areas. Choriocapillaris (CC) optical coherence tomography angiography (OCTA) in the second column. The GA areas are presented in white over CC OCTA (third column). Shadow artifacts are presented in gray over CC OCTA (fourth column). Normal CC perfusion labeled in green, GA in white, shadow artifact in gray, and LPA in red (fifth column). The flow CC density map shows lower CC density as blue area and higher CC flow density as red area (sixth column). Cross-sectional structural OCTA shows layer segmentation (seventh column).

for baseline and follow-up visit respectively. The baseline SSI and Q score was not significantly correlated with baseline CC-VD ($P = 0.13$ and 0.47 respectively). The mean annual enlargement rate of GA was 0.25 ± 0.19 mm (range = 0.05–0.57 mm). The annual GA enlargement rate was significantly associated with baseline CC-VD ($r = -0.816$, $P = 0.004$), LPA ($r = 0.809$, $P = 0.005$), and FPL ($r = 0.800$, $P = 0.005$; Figs. 2–4). The annual GA enlargement rate was not significantly associated with baseline GA area ($r = -0.362$, $P = 0.30$), SSI ($r = -0.423$, $P = 0.23$), Q score ($r = -0.16$, $P = 0.67$), age ($r = 0.008$, $P = 0.98$), axial length ($r = 0.414$, $P = 0.27$), or best correct visual acuity (BCVA; $r = -0.586$, $P = 0.08$).
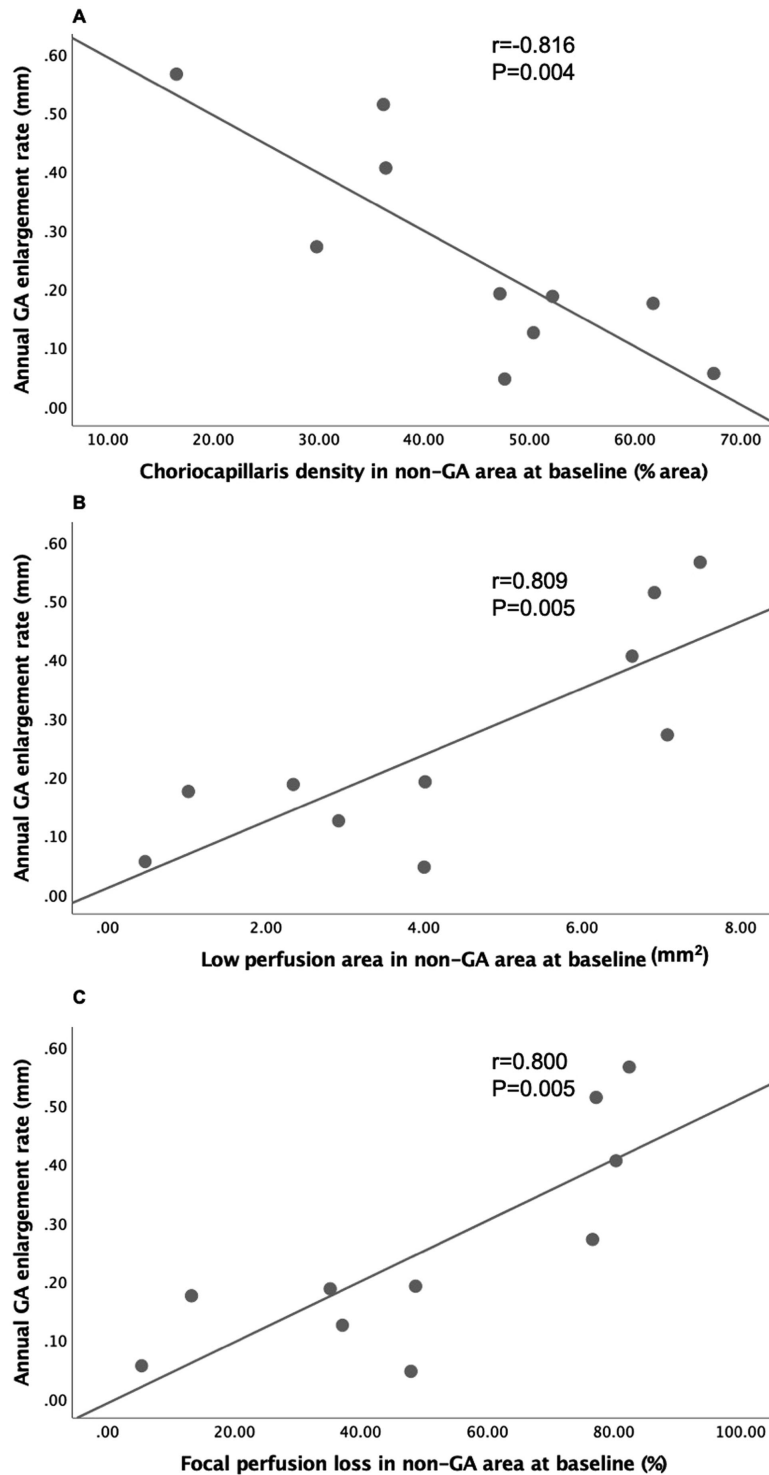
DISCUSSION

The progression rate of GA is highly variable among individual patients.[30] Understanding GA progression and its potential associations is important for clinical judgment of disease prognosis, interpretation of clinical trial results and evaluating innovative potential treatment strategies. Previous studies have reported significant associations between a higher GA enlargement rate and some clinical characteristics, such as a larger baseline lesion size, multifocal lesions, perilesional banded, or diffuse pattern fundus autofluorescence, perifoveal location, bilateral GA, and higher progression rate in fellow eye, Fleckenstein et al.[30] The current study demonstrates that, in addition to these factors, CC flow deficits, quantified with OCTA as lower CC-VD, larger LPA, and greater FPL in non-GA areas, are associated with a faster GA progression rate, suggesting perfusion impairment in choriocapillaris may be a risk factor for faster GA enlargement. Currently, clinical trials are underway to slow down GA progression. LPA, FPL, and CC-VD could be useful

in selecting clinical trial candidates. For example, a patient with larger LPA and bigger FPL may show the treatment effect more easily.

Previous studies have commonly used GA lesion area enlargement rate (mm²/year) to assess its progression.[31] Studies have consistently reported significant associations between baseline atrophic area and the area enlargement rate.[2,30–32] Mathematically, compared to a smaller baseline lesion, a larger lesion will expand with a larger area even their diameter growth rate is actually the same. In the current study, we used square root of the GA area to measure its progression rate. This limits the impact of baseline GA lesion size when evaluating GA enlargement rate associations, because square root of baseline lesion size is not significantly associated with its annual enlargement rate, as reported previously.[32] Similar methods have been used in other studies.[11] The mean annual enlargement rate of 0.25 mm/year in the current study is similar to that of Age-Related Eye Disease Study (AREDS) study (0.29 mm/year).[33] After excluding the impact of baseline GA lesion size, we found CC flow deficits in the non-GA region were significantly correlated with the annual GA enlargement rate.

Our finding that CC flow deficit is significantly associated with GA annual enlargement rate is consistent with a recent study reported by Thulliez.[11] In that study, the authors found out the GA enlargement rate correlated best with the overall average CC flow deficits in the whole non-GA region ($r = 0.747$) than the CC flow deficits in the 300 µm ($r = 0.544$) and 300–600 µm regions ($r = 0.677$) immediately surrounding the GA region, despite the highest flow deficit was found in the 300 µm rim immediately surrounding the GA. The authors speculated this finding might be due to the unevenly distribution of age-related loss of CC.

A

r=-0.816
P=0.004

Annual GA enlargement rate (mm)

Choriocapillaris density in non-GA area at baseline (% area)

B

r=0.809
P=0.005

Annual GA enlargement rate (mm)

Low perfusion area in non-GA area at baseline (mm²)

C

r=0.800
P=0.005

Annual GA enlargement rate (mm)

Focal perfusion loss in non-GA area at baseline (%)

FIGURE 4. Annual geographic atrophy enlargement rate versus baseline choriocapillaris flow deficits. The annual geographic atrophy (GA) enlargement rate significantly increased with a lower choriocapillaris density (**A**), larger low perfusion area (**B**), and greater focal perfusion loss (**C**).

Within a 5-mm circle centered on the fovea, the age-related CC perfusion loss was faster in the central foveal region than in the peripheral region.[11] However, the authors did not mention how many of their GA cases were foveal center involved and how many of their GA lesion located peri-foveal region. To avoid the impact of location on assess-ing the CC perfusion loss, we introduced the concept of LPA and FPL in the current study, which were calculated through location-wised comparison with the normal refer-ence map generated from normal controls. The correlations between the LPA or FPL and GA enlargement rates were both significant (r = 0.809 and 0.800). Similarly, Moult et al.

reported a trend of increasing GA growth rate with increasing CC impairment.[16] These results agree with the findings recently reported by Sacconi, who found out CC impairment could predict the enlargement of GA lesion, suggesting CC impairment could be considered as a new risk factor for GA progression and a biomarker to be measured to determine efficacy of new interventions aiming to slow GA progression.[13]

Our methods used in the current cohort study are slightly different from the above mentioned two longitudinal studies.[11,13] We used spectral domain OCT and applied the sophisticated artifact removal methods to improve the measurement accuracy. Although OCT signal is significantly attenuated by the highly scattering RPE, previous studies have demonstrated the OCTA signal from the CC layer is adequate to evaluate the choriocapillaris blood flow information in both spectral domain[14,22] and swept source OCT platforms.[10,11,13] CC flow measurements with either spectral domain or swept source OCT angiography is vulnerable to artifacts, such as motion, projection, segmentation errors, and shadows. Taking measures to reduce these artifacts by image processing is a critical step in attempting accurately quantify CC flow. For example, without removal of projection or bulk motion artifacts, it is easy to overestimate the CC-VD, which can mistakenly reach up to 90% to 99%.[34,35] Applying projection resolved OCTA and accounting for bulk motion, our result of CC-VD 80% in normal controls approximates the value of 75% reported in histology.[36] Shadow artifacts from iris, floaters, retinal vessels, and drusen could attenuate CC signal, leading to an artifactually low CC-VD value. In the current study, we used a supervised machine learning algorithm to analyze the interaction between reflectance and flow signal to detect shadows objectively and reliably.[22,26] The ICC for intra-visit repeat scans was 0.958, 0.947, and 0.955 for CC-VD, LPA, and FPL measurements, respectively, demonstrating excellent repeatability for these measurements.

The small sample size of the current study limits our ability to perform multivariate analysis to adjust the impact of other known risk factors of GA progression, such as fundus autofluorescence pattern, fellow eye status, and reticular pseudodrusen. Nevertheless, with normalization of the baseline lesion size by using square root and the location-wise comparison with normal healthy controls, we found out CC flow deficits in the non-GA region is associated with a faster annual GA enlargement rate. The advantage of the current study is the application of novel algorithms that improve the accuracy of CC measurements. Additionally, we accounted for the uneven distribution of age-related CC loss by comparing macular regions with attenuated CC perfusion in eyes with GA to similar macular regions in control eyes.

In conclusion, CC flow deficits, quantified with OCTA as lower CC-VD, larger LPA, or greater FPL in non-GA areas were significantly associated with a faster GA enlargement, suggesting the choriocapillaris perfusion outside of the GA area may play a role in GA progression.

Disclosure: **Q.S. You**, None; **A. Camino**, Optovue Inc. (P); **J. Wang**, None; **Y. Guo**, None; **C.J. Flaxel**, None; **T.S. Hwang**, None; **D. Huang**, Optovue Inc. (F, I, P, R); **Y. Jia**, Optovue Inc. (F, P); **S.T. Bailey**, Optovue Inc. (F)

References

1. Lim LS, Mitchell P, Seddon JM, Holz FG, Wong TY. Age-related macular degeneration. *Lancet (London, England)*. 2012;379(9827):1728–1738.

2. Schmitz-Valckenberg S, Sahel JA, Danis R, et al. Natural History of Geographic Atrophy Progression Secondary to Age-Related Macular Degeneration (Geographic Atrophy Progression Study). *Ophthalmology*. 2016;123(2):361–368.

3. Holz FG, Strauss EC, Schmitz-Valckenberg S, van Lookeren Campagne M. Geographic atrophy: clinical features and potential therapeutic approaches. *Ophthalmology*. 2014;121(5):1079–1091.

4. Lindblad AS, Lloyd PC, Clemons TE, et al. Change in area of geographic atrophy in the Age-Related Eye Disease Study: AREDS report number 26. *Arch Ophthalmol (Chicago, IL : 1960)*. 2009;127(9):1168–1174.

5. Clemons TE, Milton RC, Klein R, Seddon JM, Ferris FL, 3rd. Risk factors for the incidence of Advanced Age-Related Macular Degeneration in the Age-Related Eye Disease Study (AREDS) AREDS report no. 19. *Ophthalmology*. 2005;112(4):533–539.

6. Chew EY, Clemons TE, Agrón E, et al. Long-term effects of vitamins C and E, *β*-carotene, and zinc on age-related macular degeneration: AREDS report no. 35. *Ophthalmology*. 2013;120(8):1604–1611.e4.

7. Coleman DJ, Silverman RH, Rondeau MJ, Lloyd HO, Khanifar AA, Chan RV. Age-related macular degeneration: choroidal ischaemia? *Br J Ophthalmol*. 2013;97(8):1020–1023.

8. Seddon JM, McLeod DS, Bhutto IA, et al. Histopathological Insights Into Choroidal Vascular Loss in Clinically Documented Cases of Age-Related Macular Degeneration. *JAMA Ophthalmol*. 2016;134(11):1272–1280.

9. Jia Y, Tan O, Tokayer J, et al. Split-spectrum amplitude-decorrelation angiography with optical coherence tomography. *Optics Express*. 2012;20(4):4710–4725.

10. Nassisi M, Shi Y, Fan W, et al. Choriocapillaris impairment around the atrophic lesions in patients with geographic atrophy: a swept-source optical coherence tomography angiography study. *Br J Ophthalmol*. 2019;103(7):911–917.

11. Thulliez M, Zhang Q, Shi Y, et al. Correlations between Choriocapillaris Flow Deficits around Geographic Atrophy and Enlargement Rates Based on Swept-Source OCT Imaging. *Ophthalmol Retina*. 2019;3(6):478–488.

12. You QS, Wang J, Guo Y, et al. Detection of Reduced Retinal Vessel Density in Eyes with Geographic Atrophy Secondary to Age-Related Macular Degeneration Using Projection-Resolved Optical Coherence Tomography Angiography. *Am J Ophthalmol*. 2020;209:206–212.

13. Sacconi R, Corbelli E, Borrelli E, et al. Choriocapillaris flow impairment could predict the enlargement of geographic atrophy lesion. *Br J Ophthalmol*. 2021;105:97–102.

14. Sacconi R, Corbelli E, Carnevali A, Querques L, Bandello F, Querques G. Optical coherence tomography angiography in geographic atrophy. *Retina (Philadelphia, Pa)*. 2018;38(12):2350–2355.

15. Moult EM, Waheed NK, Novais EA, et al. Swept-source optical coherence tomography angiography reveals choriocapillaris alterations in eyes with nascent geographic atrophy and drusen-associated geographic atrophy. *Retina (Philadelphia, Pa)*. 2016;36(Suppl 1):S2–S11.

16. Moult EM, Alibhai AY, Lee B, et al. A Framework for Multiscale Quantitation of Relationships Between Choriocapillaris Flow Impairment and Geographic Atrophy Growth. *Am J Ophthalmol*. 2020;214:172–187.

17. Gao SS JY, Huang D. Artifacts in Optical Coherence Tomography Angiography. In: Huang D, Lumbroso B, Jia Y, Waheed N , editors. *Optical Coherence Tomography Angiography of the Eye*. Thorofare, NJ: SLACK Publishing; 2017; 33–40.

18. Camino A, Jia Y, Liu G, Wang J, Huang D. Regression-based algorithm for bulk motion subtraction in optical coherence tomography angiography. *Biomed Optics Express*. 2017;8(6):3053–3066.

19. Wang J, Zhang M, Hwang TS, et al. Reflectance-based projection-resolved optical coherence tomography angiography [Invited]. *Biomed Optics Express*. 2017;8(3):1536–1548.

20. Alten F, Lauermann JL, Clemens CR, Heiduschka P, Eter N. Signal reduction in choriocapillaris and segmentation errors in spectral domain OCT angiography caused by soft drusen. *Graefes Arch Clin Exp Ophthalmol*. 2017;255(12):2347–2355.

21. Ghasemi Falavarjani K, Al-Sheikh M, Akil H, Sadda SR. Image artefacts in swept-source optical coherence tomography angiography. *Br J Ophthalmol*. 2017;101(5):564–568.

22. Camino A, Guo Y, You Q, et al. Detecting and measuring areas of choriocapillaris low perfusion in intermediate, non-neovascular age-related macular degeneration. *Neurophotonics*. 2019;6(4):041108.

23. Gao SS, Patel RC, Jain N, et al. Choriocapillaris evaluation in choroideremia using optical coherence tomography angiography. *Biomedical Optics Express*. 2017;8(1):48–56.

24. Zhang M, Hwang TS, Campbell JP, et al. Projection-resolved optical coherence tomographic angiography. *Biomed Optics Express*. 2016;7(3):816–828.

25. Zhang M, Wang J, Pechauer AD, et al. Advanced image processing for optical coherence tomographic angiography of macular diseases. *Biomed Optics Express*. 2015;6(12):4661–4675.

26. Camino A, Jia Y, Yu J, Wang J, Liu L, Huang D. Automated detection of shadow artifacts in optical coherence tomography angiography. *Biomed Optics Express*. 2019;10(3):1514–1531.

27. Kurokawa K, Liu Z, Miller DT. Adaptive optics optical coherence tomography angiography for morphometric analysis of choriocapillaris [Invited]. *Biomed Optics Express*. 2017;8(3):1803–1822.

28. Zhao R, Camino A, Wang J, et al. Automated drusen detection in dry age-related macular degeneration by multiple-depth, en face optical coherence tomography. *Biomed Optics Express*. 2017;8(11):5049–5064.

29. Sadda SR, Guymer R, Holz FG, et al. Consensus Definition for Atrophy Associated with Age-Related Macular Degeneration on OCT: Classification of Atrophy Report 3. *Ophthalmology*. 2018;125(4):537–548.

30. Fleckenstein M, Mitchell P, Freund KB, et al. The Progression of Geographic Atrophy Secondary to Age-Related Macular Degeneration. *Ophthalmology*. 2018;125(3):369–390.

31. Sadda SR, Chakravarthy U, Birch DG, Staurenghi G, Henry EC, Brittain C. Clinical endpoints for the study of geographic atrophy secondary to age-related macular degeneration. *Retina (Philadelphia, Pa)*. 2016;36(10):1806–1822.

32. Feuer WJ, Yehoshua Z, Gregori G, et al. Square root transformation of geographic atrophy area measurements to eliminate dependence of growth rates on baseline lesion measurements: a reanalysis of age-related eye disease study report no. 26. *JAMA Ophthalmology*. 2013;131(1):110–111.

33. Domalpally A, Danis R, Agrón E, Blodi B, Clemons T, Chew E. Evaluation of Geographic Atrophy from Color Photographs and Fundus Autofluorescence Images: Age-Related Eye Disease Study 2 Report Number 11. *Ophthalmology*. 2016;123(11):2401–2407.

34. Nassisi M, Lavia C, Alovisi C, Musso L, Eandi CM. Short-Term Choriocapillaris Changes in Patients with Central Serous Chorioretinopathy after Half-Dose Photodynamic Therapy. *Int J Mol Sci*. 2017;18(11):2468.

35. Alten F, Heiduschka P, Clemens CR, Eter N. Exploring choriocapillaris under reticular pseudodrusen using OCT-Angiography. *Graefes Arch Clin Exp Ophthalmol*. 2016;254(11):2165–2173.

36. Ramrattan RS, van der Schaft TL, Mooy CM, de Bruijn WC, Mulder PG, de Jong PT. Morphometric analysis of Bruch's membrane, the choriocapillaris, and the choroid in aging. *Invest Ophthalmol Vis Sci*. 1994;35(6):2857–2864.